The Journal of Immunology

RESEARCH ARTICLE | JUNE 15 2013

TLR3-Triggered Reactive Oxygen Species Contribute to Inflammatory Responses by Activating Signal Transducer and Activator of Transcription-1

FREE

Chul-Su Yang; ... et. al

J Immunol (2013) 190 (12): 6368–6377.
https://doi.org/10.4049/jimmunol.1202574

TLR3-Triggered Reactive Oxygen Species Contribute to Inflammatory Responses by Activating Signal Transducer and Activator of Transcription-1

Chul-Su Yang,*,† Jwa-Jin Kim,*,† Sung Joong Lee,‡ Jung Hwan Hwang,§ Chul-Ho Lee,§ Myung-Shik Lee,¶ and Eun-Kyeong Jo*,†,‖

Intracellular reactive oxygen species (ROS) are essential secondary messengers in many signaling cascades governing innate immunity and cellular functions. TLR3 signaling is crucially involved in antiviral innate and inflammatory responses; however, the roles of ROS in TLR3 signaling remain largely unknown. In this study, we show that TLR3-induced ROS generation is required for the activation of NF-κB, IFN-regulatory factor 3, and STAT1-mediated innate immune responses in macrophages. TLR3 induction led to a rapid increase in ROS generation and a physical association between components of the NADPH oxidase (NOX) enzyme complex (NOX2 and p47^{phox}) and TLR3 via a Ca^{2+}-c-Src tyrosine kinase–dependent pathway. TLR3-induced ROS generation, NOX2, and p47^{phox} were required for the phosphorylation and nuclear translocation of STAT1 and STAT2. TLR3-induced activation of STAT1 contributed to the generation of inflammatory mediators, which was significantly attenuated in NOX2- and p47^{phox}-deficient macrophages, suggesting a role for ROS-STAT1 in TLR3-mediated innate immune responses. Collectively, these results provide a novel insight into the crucial role that TLR3-ROS signaling plays in innate immune responses by activating STAT1. ***The Journal of Immunology*****, 2013, 190: 6368–6377.**

Toll-like receptors are a family of innate immune-recognition receptors that recognize molecular patterns associated with microbial pathogens and induce antimicrobial immune responses. TLR3 is recognized by dsRNA and its synthetic analog polyinosinic-polycytidylic acid (poly(I:C)), potent stimulators of type 1 IFN production (1). Interactions between TLRs and microbial structures present in pathogens mediate a signaling cascade that culminates in the upregulation of proinflammatory pathways (2). The signaling pathway activated by ligation of TLR3 involves an adaptor molecule, Toll/IL-1R domain–containing adaptor inducing IFN-β (TRIF) (3), whereas other TLRs use the adaptor molecule MyD88 in their signaling activation (4). TLR3-dependent signaling leads to the production of inflammatory cytokines and IFN regulatory factor (IRF)-3 activation through the recruitment of TRIF/TICAM-1 to TLR3. This induces type I IFN production and subsequently the induction of IFN-responsive genes such as antiviral genes and that encoding CXC chemokine IP-10/CXCL10 (5, 6).

The type I IFNs instigate an autocrine/paracrine loop and lead to the sequential activation of JAK and STAT proteins, and are thus able to regulate pleiotropic biological functions in different types of cells (7). Additionally, the activation of the transcription factor STAT1 plays a major role in the transcriptional activation of type I IFNs (IFN-α/β) (8). Moreover, STAT1 signaling plays a critical role in intracellular redox signaling in activated macrophages (9). Interactions among STATs through reciprocal SH2 domain/phosphotyrosine binding results in the formation of transcription factor complexes. The STAT1 homodimer is active as a transcription factor and binds to different DNA sequences, known as IFN-γ–activated site elements (10, 11). Activation of the transcription factor STAT1, NF-κB, and Sp-1 plays a major role in the transcriptional activation of type I IFNs (IFN-α/β), TNF-α, and IL-10, respectively (8). STAT1 complexes cooperate with NF-κB to induce full transcriptional activation of many antiviral genes that are detrimental to virus survival (12).

Emerging evidence suggests that reactive oxygen species (ROS) contribute to diverse signaling processes, including TLR-induced innate immune responses, autophagy, and inflammation (13–15). It has been demonstrated that gp91^{phox}/NADPH oxidase (NOX)2 plays an essential role in TLR2-dependent inflammatory responses and antimicrobial activity against mycobacteria (16). Additionally, TLR4-dependent ROS generation is essential for mammalian innate immunity by acting through the TRAF6/ASK1/p38 axis (17). However, the roles of ROS in the regulation of TLR3-dependent intracellular signaling and innate immune responses are largely uncharacterized. In this study, we investigated the roles

*Department of Microbiology, Chungnam National University, Daejeon 301-747, South Korea; †Infection Signaling Network Research Center, Chungnam National University, Daejeon 301-747, South Korea; ‡Department of Oral Physiology, School of Dentistry, Seoul National University, Seoul 110-768, South Korea; §Laboratory Animal Center, Korea Research Institute of Bioscience and Biotechnology, Daejeon 305-806, South Korea; ¶Department of Medicine, Samsung Medical Center, Sungkyunkwan University School of Medicine, Seoul 135-710, South Korea; and ‖Research Institute for Medical Sciences, College of Medicine, Chungnam National University, Daejeon 301-747, South Korea

Received for publication September 13, 2012. Accepted for publication April 4, 2013.

This work was supported by a National Research Foundation of Korea grant funded by the Korean Ministry of Science and Technology through Infection Signaling Network Research Center Grant 2007-0054932 at Chungnam National University, as well as by the Korea Research Institute of Bioscience and Biotechnology Research Initiative Program.

Address correspondence and reprint requests to Dr. Eun-Kyeong Jo, Department of Microbiology, College of Medicine, Chungnam National University, 6 Munhwa-dong, Jungku, Daejeon 301-747, South Korea. E-mail address: hayoungj@cnu.ac.kr

The online version of this article contains supplemental material.

Abbreviations used in this article: BMDM, bone marrow–derived macrophage; CGD, chronic granulomatous disease; DHE, dihydroethidium; DPI, diphenylene iodonium; IKK, IκB kinase; iNOS, inducible NO synthase; IRF, IFN regulatory factor; KO, knockout; NAC, *N*-acetylcysteine; NOX, NADPH oxidase; poly(I:C), polyinosinic-polycytidylic acid; PP1, 4-amino-5-(4-methylphenyl)-7-(*t*-butyl)pyrazolo[3,4-*d*]-pyrimidine; PP2, 4-amino-5-(4-chlorophenyl)-7-(*t*-butyl)pyrazolo[3,4-*d*]pyrimidine; PP3, 4-amino-7-phenylpyrazolo[3,4-*d*] pyrimidine; ROS, reactive oxygen species; siNS, nonspecific small interfering RNA; siRNA, small interfering RNA; TRIF, Toll/IL-1R domain–containing adaptor inducing IFN-β; WT, wild-type.

of TLR3-induced ROS-STAT1 signaling in innate immune responses, as well as the mechanisms by which TLR3 can trigger ROS generation in macrophages. We found that TLR3-dependent ROS generation is essential for the activation of NF-κB, IRF-3, and STAT1, and it enhances the release of inflammatory mediators. TLR3 stimulation led to a physical and functional association between components of the NOX enzyme complex (NOX2 and $p47^{phox}$) and TLR3. The generation of NOX2-dependent ROS and NOX2 association with TLR3 were dependent on the activation of c-Src tyrosine kinase and intracellular Ca^{2+} release. TLR3-dependent ROS generation was required for the phosphorylation and nuclear translocation of STAT1 and STAT2. Furthermore, activation of TLR3-induced ROS and STAT1 was crucial for the release of antiviral inflammatory mediators, including chemokines and NO. These data provide novel insight into the role of TLR3-ROS signaling in innate immune responses through activation of STAT1.

Materials and Methods

Mice and cells

Primary bone marrow–derived macrophages (BMDMs) were prepared from 6- to 8-wk-old female NOX2, $p47^{phox}$, TLR3, TRIF, and STAT1 knockout (KO) mice (on the C57BL/6 background), as described previously (16, 18). Briefly, bone marrow cells from the femur and tibia were cultured for 4–5 d in DMEM (Life Technologies BRL) containing M-CSF (25 ng/ml), 4 mM glutamine, and 10% FBS. After culture, the BMDMs were washed vigorously to remove nonadherent cells and then were used in the desired assay. Peritoneal macrophages were isolated from 4% thioglycollate-elicited peritoneal exudate cells and purified by adherence. The adherent monolayer was incubated in DMEM with 2% FBS under experimental or control conditions for the indicated times before assay. All animals were maintained in a pathogen-free environment. All experimental procedures were reviewed and approved by the Institutional Animal Care and Use Committee of Chungnam National University. The mouse macrophage cell line RAW264.7 (ATCC TIB-71; American Type Culture Collection) was maintained in DMEM (Invitrogen) containing 10% FBS (Invitrogen), sodium pyruvate, nonessential amino acids, penicillin G (100 IU/ml), and streptomycin (100 μg/ml).

Reagents, DNA, and Abs

The poly(I:C) and LPS (*Escherichia coli* 0111:B4) used for the in vitro assay were purchased from Sigma-Aldrich. BAPTA-AM, 4-amino-5-(4-methylphenyl)-7-(*t*-butyl)pyrazolo[3,4-*d*]-pyrimidine (PP1), 4-amino-5-(4-chlorophenyl)-7-(*t*-butyl)pyrazolo[3,4-*d*]pyrimidine (PP2), 4-amino-7-phenylpyrazolo[3,4-*d*] pyrimidine (PP3), *N*-acetylcysteine (NAC), diphenylene iodonium (DPI), pyrrolidine dithiocarbamate ammonium, 4-(2-aminoethyl)-benzenesulfonyl fluoride hydrochloride, and allopurinol were purchased from Calbiochem. A rat anti-mouse IFN-α mAb (clone RMMA-1, IgG1), a rat anti-mouse IFN-β mAb (clone RMMB-1, IgG1), and an isotype control mAb (IgG1) was purchased from PBL Interferon Source. DMSO (Sigma-Aldrich) was added to the cultures at a concentration of 0.1% (v/v) as a solvent control. The NF-κB luciferase reporter plasmid was a gift from Dr. G.M. Hur (Chungnam National University, Daejeon, south Korea). The mouse RIG-I, MDA5, c-Src, and STAT1 small interfering RNAs (siRNAs; Santa Cruz Biotechnology) were a pool of three target-specific siRNAs (20–25 nt in length) designed to knock down gene expression. The cells were transfected using Lipofectamine 2000 (Invitrogen), as indicated by the manufacturer. Specific Abs against c-Src, phospho-(Tyr^{416})-c-Src, STAT1, phospho-(Tyr^{701})-STAT1, phospho-(Ser^{727})-STAT1, STAT2, phospho-(Tyr^{690})-STAT2, and phospho-IκB kinase (IKK)α/β were purchased from Cell Signaling Technology. Abs specific for α-actin (I-19), IκB-α (C-21), NOX2 (G-1), TLR3 (H-125), $p47^{phox}$ (H-195), IRF-3 (FL-425), lamin B1 (H-90), and NF-κB p65 (C-20) were purchased from Santa Cruz Biotechnology. Cy2-conjugated anti-mouse, rhodamine (tetramethylrhodamine isothiocyanate)-conjugated anti-rabbit, and PE-conjugated anti-mouse Abs were purchased from Jackson ImmunoResearch Laboratories.

Western blotting and coimmunoprecipitation

RAW264.7 cells and BMDMs were treated as indicated and processed for analysis by Western blotting and immunoprecipitation, as previously described (16). For Western blot analysis, primary Abs were used at a 1:1000 dilution. The membranes were developed using a chemiluminescence assay (ECL; Amersham Pharmacia) and were subsequently exposed to chemiluminescence film (Amersham Pharmacia). For the immunoprecipitation assays, RAW264.7 cells were harvested and lysed with Nonidet P-40 buffer (50 mM HEPES [pH 7.4], 150 mM NaCl, 1 mM EDTA, 1% [v/v] Nonidet P-40) containing 1% CHAPS and supplemented with a complete protease inhibitor mixture (Roche). The lysates were mixed and precipitated with Abs and protein A-Sepharose by incubation at 4°C for 18 h on a rotator. The samples were subsequently solubilized in SDS sample buffer and separated by SDS-PAGE for Western blot analysis.

Subcellular fractionation and detection of nuclear translocation

Cell stimulation was terminated by the addition of ice-cold PBS, and nuclear and cytosolic protein extracts were prepared using a nuclear extraction kit (Active Motif, Carlsbad, CA), according to the manufacturer's instructions. All steps of subcellular fractionation were carried out at 4°C. Fraction purity was tested by Western blotting using actin as a cytoplasmic marker and lamin B1 as a nuclear marker.

RNA extraction and RT-PCR

Total RNA was extracted using TRIzol reagent (Invitrogen), as described previously (18). Total RNA (2 μg) was used for first-strand cDNA synthesis with Moloney murine leukemia virus reverse transcriptase (Promega), according to the manufacturer's instructions. The PCR conditions were as described previously (18). The primer pairs used for PCR are listed in Supplemental Table I. PCR products were resolved on 1.5% agarose gels and were stained with ethidium bromide.

Immunofluorescence and confocal analysis

The cells were fixed on coverslips with 4% (w/v) paraformaldehyde in PBS and then permeabilized through incubation for 10 min with 0.25% (v/v) Triton X-100 in PBS at 25°C. NF-κB p65, STAT1, or IRF-3 was detected through incubation with a 1:100 dilution of the primary Ab for 1 h at 25°C. After washing, the secondary Abs were added and the cells were incubated in 1% BSA/PBS buffer for 30 min. The nuclei were visualized following incubation for 15 min with 1 μg/ml DAPI (Sigma-Aldrich). The slides were examined using an LSM 510 laser-scanning confocal microscope (Zeiss, Oberkochen, Germany).

Intracellular Ca^{2+} measurements

BMDMs grown on coverslips were loaded with the Ca^{2+} indicator Fluo-4/AM (10 μM; Molecular Probes) in HBSS for 30 min, according to the manufacturer's protocol. Confocal images were obtained using an LSM 510 confocal microscope (Zeiss), with an excitation wavelength of 488 nm (argon laser) and emission at 500–550 nm.

Determination of NF-κB and IRF-3 DNA binding activities

Nuclear extracts were prepared as previously described (18). IRF-3 and NF-κB DNA-binding activities in nuclear extracts were measured using Trans-AM IRF-3 and p65 transcription factor assay kits, respectively (Active Motif Europe, Rixensart, Belgium), according to the manufacturer's protocols. Briefly, 5 μg nuclear extract was incubated in plates coated with consensus IFN-stimulated response elements and NF-κB oligonucleotides. Plates were washed and anti–IRF-3 or p65 Abs were added to the wells. Ab binding was detected with a secondary HRP-conjugated Ab, and the signal was developed with tetramethylbenzidine substrate. The intensity of the signal at 450 nm was measured.

Measurement of intracellular ROS

Intracellular ROS levels were measured using the oxidative fluorescent dye dihydroethidium (DHE; Calbiochem), as previously described (16, 18). Cells were examined with an LSM 510 laser scanning confocal microscope (Zeiss), and the mean relative fluorescence intensity for each group of cells was measured with the Zeiss LSM 510 vision system (version 2.3). Intracellular ROS levels were also measured by flow cytometry using a FACSCalibur flow cytometer (BD Biosciences, San Jose, CA). The data were plotted using CellQuest software (BD Biosciences).

Intracellular superoxide production was measured by the lucigenin (bis-*N*-methylacridinium nitrate)-ECL method, as described previously (16, 18). Briefly, cells were allowed to equilibrate for 30 min at 37°C in a reaction mixture containing 50 mM phosphate buffer (pH 7.0), 1 mM EGTA, 150 mM sucrose, and a protease inhibitor mixture prior to the addition of Krebs-HEPES buffer containing lucigenin (5 μM) as the electron acceptor and NADPH (100 μM) as the electron donor. The values are expressed as relative light units per 1×10^5 cells.

Statistical analysis

All data were analyzed by a Student *t* test with Bonferroni adjustment or by ANOVA for multiple comparisons and are presented as the means ± SD. Differences were considered significant at $p < 0.05$.

Results

TLR3-TRIF signaling triggers intracellular ROS generation in macrophages

It has been demonstrated that intracellular ROS is required in TLR2- (16, 19) and TLR4-dependent inflammatory responses (17). However, TLR3-ROS signaling remains largely uncharacterized. We first determined whether stimulation with poly(I:C), a synthetic dsRNA analog, leads to ROS generation in murine BMDMs in a TLR3-dependent manner. To achieve this, we treated murine BMDMs with poly(I:C) and measured the generation of ROS by staining with the oxidative fluorescent dye DHE to detect superoxide production. As shown in Fig. 1A, poly(I:C) induced a robust burst of ROS production in wild-type macrophages within 30 min of stimulation (Fig. 1A). However, TLR3-induced ROS generation was markedly inhibited in BMDMs from NOX2 KO and $p47^{phox}$ KO mice (Fig. 1B).

We next examined whether poly(I:C)-triggered ROS production depends on TLR3 and TRIF, an essential adaptor of TLR3 signaling (5, 6). As shown in Fig. 1C and 1D, poly(I:C)-mediated ROS production was markedly attenuated in BMDMs from TLR3 and TRIF KO mice, as compared with those from WT mice. However, LPS-induced ROS generation was not decreased in TLR3 KO and WT cells, but it was significantly decreased in TRIF KO cells (Fig. 1D). Similar results were obtained using TLR3 siRNA-transfected RAW264.7 cells (data not shown). Thus, TLR3-TRIF signaling appears to be required for poly(I:C)-induced ROS production in macrophages. We further examined the roles of RIG-I and MDA5, key cytoplasmic helicases implicated in viral dsRNA recognition (20), in ROS generation triggered by poly(I:C) recognition. To investigate this, *RigI* and *Mda5* were knocked down in RAW264.7 cells by transfection of siRNA specific for *RigI* or *Mda5*, before transfection with poly(I:C). No significant differences were detected in poly(I:C)-induced ROS production between RAW264.7 cells transfected with scrambled control nonspecific siRNA (siNS) and cells transfected with siRNA specific for *RigI* or *Mda5* (Fig. 1E). Taken together, these results indicate that poly(I:C)-induced ROS generation is mediated by TLR3, but not by RIG-I or MDA5.

TLR3-induced ROS generation is mediated by intracellular Ca^{2+}–dependent Src kinase activation in macrophages

The tyrosine kinase c-Src is activated by dsRNA and is essential for TLR3-induced antiviral responses (21). We next examined whether TLR3 stimulation induced the activation of c-Src. The results showed that phosphorylation of c-Src at Tyr^{416} peaked within 20 min in murine BMDMs (Fig. 2A). Poly(I:C)-induced c-Src activation was attenuated by the c-Src kinase inhibitors PP1 and PP2, but not by PP3, an inactive analog (Fig. 2B). c-Src can translocate to the plasma membrane and initiate the TLR2-associated signaling involved in Ca^{2+} release (22). We thus examined intracellular Ca^{2+} influx in BMDMs in response to poly(I:C) treatment. As shown in Fig. 2C, Ca^{2+} fluxes were generated in BMDMs loaded with Fluo-4/AM after treatment with poly(I:C). We then examined whether Ca^{2+}-dependent signaling is involved in the c-Src activation induced by poly(I:C). Blocking Ca^{2+} signaling with BAPTA-AM, an intracellular calcium chelator, dose-dependently inhibited poly(I:C)-induced c-Src phosphorylation (Fig. 2D).

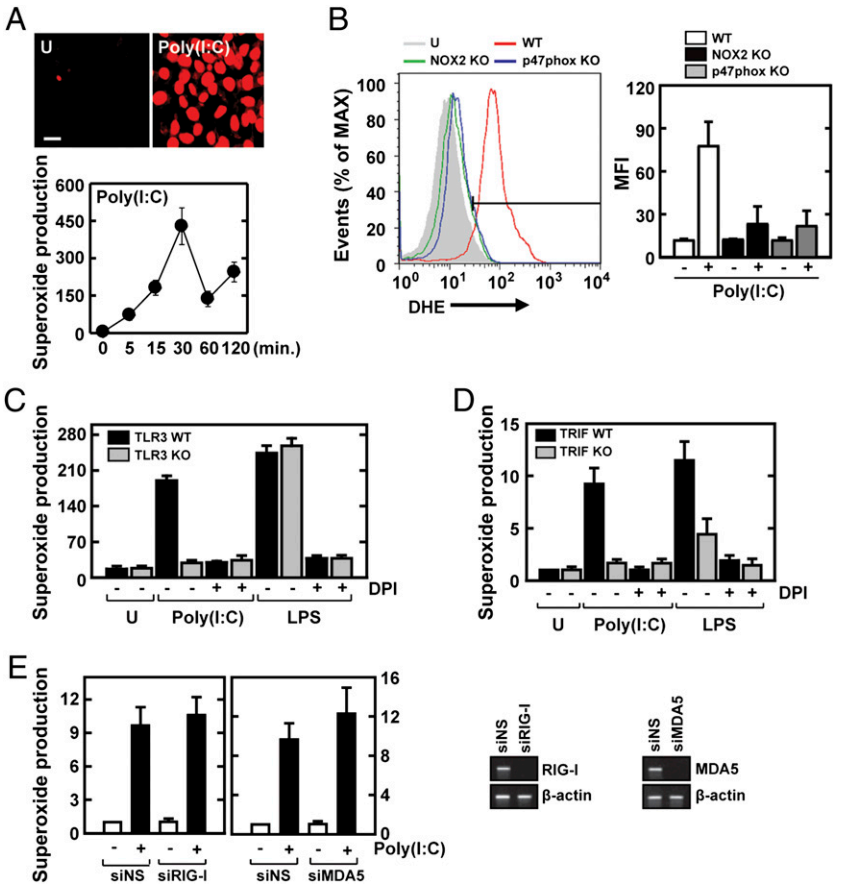

FIGURE 1. Poly(I:C) induces intracellular ROS generation in a TLR3- and TRIF-dependent manner. (**A**) DHE fluorescence intensities of BMDMs. BMDMs from WT mice were stimulated with poly (I:C) (25 μg/ml) for the indicated lengths of time. *Upper*, Images are representative of three independent experiments with similar results. Scale bar, 20 μm. (**B**) BMDMs were stimulated with poly(I:C) for 30 min, stained with DHE, and subjected to flow cytometric analysis. *Left*, Representative histogram. *Right*, Data presented as the average mean fluorescence intensity (MFI). (**C**) BMDMs were preincubated with DPI (20 μM) for 45 min before stimulation with poly(I:C) (25 μg/ml) or LPS (100 ng/ml) for 30 min. The cells were then stained and visualized by confocal microscopy. (**D**) Superoxide production was measured in BMDMs from WT and TRIF KO mice using a lucigenin-derived ECL assay. BMDMs were preincubated with DPI (20 μM) for 45 min before stimulation with poly(I:C) or LPS for 30 min. (**E**) Effects of *RigI* or *Mda5* silencing on poly(I:C)-induced superoxide production in RAW264.7 cells. Cells were transfected with siRNA targeting of RIG-I (siRIG-I) or MDA5 (siMDA5) or with siNS using Lipofectamine 2000. At 48 h after transfection, the cells were treated with poly(I:C) for 1 h. Superoxide generation was quantified using a lucigenin-derived ECL assay. *Right*, Efficacy of siRNA targeting of *RigI* or *Mda5*. The mRNA loading was normalized according to β-actin expression in cells. Quantitative data are shown as the means ± SD of three experiments (A, *lower*, B–E). U, Untreated.

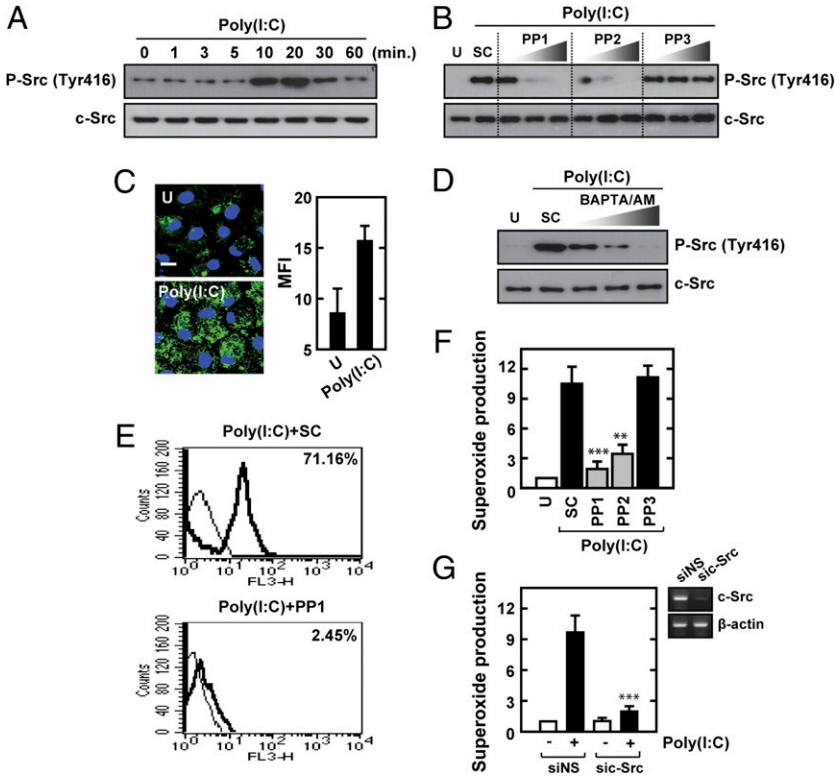

FIGURE 2. Poly(I:C)-induced generation of intracellular ROS is mediated through intracellular Ca^{2+}–dependent Src kinase activation. (**A** and **B**) Poly(I:C)-induced c-Src kinase activation. BMDMs were stimulated with poly(I:C) (25 μg/ml) for the indicated lengths of time (A) or for 20 min (B). In (B), cells were preincubated with PP1 (5, 10, or 20 μM), PP2 (5, 10, or 20 μM), or PP3 (5, 10, or 20 μM) for 45 min. The cells were then harvested and subjected to Western blotting for phosphorylated c-Src (Tyr^{416}) and c-Src (as a loading control). (**C**) Intracellular Ca^{2+} influx. BMDMs were stimulated with poly(I:C) for 5 min and were then loaded with Fluo-4/AM and subjected to confocal microscopic analysis. Scale bar, 20 μm. *Right*, Average mean fluorescence intensity (MFI). (**D**) Poly(I:C) induced c-Src kinase activation in a Ca^{2+}-dependent manner. BMDMs were preincubated with BAPTA-AM (5, 10, or 25 μM) for 45 min and then stimulated with poly(I:C) for 20 min. The cells were then harvested and subjected to Western blotting for phosphorylated c-Src (Tyr^{416}) and c-Src (as a loading control). (**E**–**G**) Poly(I:C) induced ROS generation in an Src kinase–dependent manner. (E) Representative data for intracellular ROS levels as determined by DHE staining and flow cytometric analysis. BMDMs were stimulated with poly(I:C) for 30 min in the presence or absence of PP1 (10 μM) for 45 min. (F) BMDMs were stimulated with poly(I:C) for 30 min in the presence or absence of PP1 (10 μM), PP2 (10 μM), or PP3 (10 μM) for 45 min. Intracellular ROS generation was quantified using a lucigenin-derived ECL assay. (G) RAW264.7 cells were transfected with siRNA targeting of *c-Src* (sic-Src) or siNS using Lipofectamine 2000. At 48 h after transfection, the cells were stimulated with poly(I:C) for 30 min. Intracellular ROS generation was quantified using a lucigenin-derived ECL assay. *Right*, Efficacy of the siRNA targeting of *c-Src*. The mRNA loading was normalized according to β-actin expression in cells. Data (A, B, C, *left*, D, E) are representative of at least three independent experiments with similar results. Quantitative data are shown as the means ± SD of three experiments (C, *right*, F, G). $***p < 0.001$, compared with solvent control. SC, Solvent control (0.1% DMSO); U, untreated.

Because the data above showed that TLR3 stimulation induced ROS generation and c-Src activation, we further examined whether c-Src is required for poly(I:C)-dependent ROS generation. Selective inhibition of c-Src using pharmacological inhibitors (PP1 and PP2) substantially decreased TLR3-dependent ROS generation (Fig. 2E, 2F). To further evaluate the role of c-Src in TLR3-mediated ROS generation, c-Src was silenced in RAW264.7 cells by transfection with siRNA specific for *c-Src*, and the cells were then stimulated with poly(I:C). Data showed significantly reduced ROS generation in RAW264.7 cells by transfected with siRNA specific for *c-Src* compared with cells transfected with siNS (Fig. 2G). These results indicate that TLR3-induced ROS generation requires a Ca^{2+}/c-Src tyrosine kinase–dependent pathway.

TLR3 associates with NOX2 and p47^{phox} via intracellular Ca^{2+}–dependent c-Src in macrophages

Previous studies showed that TLR2 physically and functionally interacts with NOX2 to activate innate immune responses against mycobacteria (16). Because the data above indicate that TLR3-dependent ROS generation is mediated by Src activation, we further investigated whether TLR3 associates with NOX2 in an Src-dependent manner. The interaction between endogenous NOX2 and TLR3 was assessed in RAW264.7 macrophage cells by immunoprecipitation experiments with anti-TLR3 and anti-NOX2 Abs. As shown in Fig. 3A, NOX2 associates with TLR3 transiently (from 15 to 30 min). No further association was detected during prolonged incubation with poly(I:C). Endogenous TLR3 was able to specifically pull down NOX2 from cell lysates of RAW264.7 macrophages stimulated with poly(I:C). Similarly, TLR3 was also detected in the immunoprecipitates of endogenous NOX2 (Fig. 3A).

We next examined whether intracellular Ca^{2+} and c-Src tyrosine kinase contribute to the interaction of TLR3 with NOX2. As shown in Fig. 3B and 3C, pharmacologic inhibitors of intracellular Ca^{2+} (BAPTA-AM) and c-Src kinases (PP1 and PP2) significantly inhibited the poly(I:C)-induced interaction between NOX2 and TLR3, whereas PP3 had no significant effect. These data were further confirmed using RAW264.7 cells transfected with siRNA specific for c-Src or siNS. Consistent with the findings shown in Fig. 3C, specific silencing of *c-Src* resulted in marked inhibition of the poly(I:C)-induced association of NOX2 with TLR3; siNS did not show such an effect (Fig. 3D).

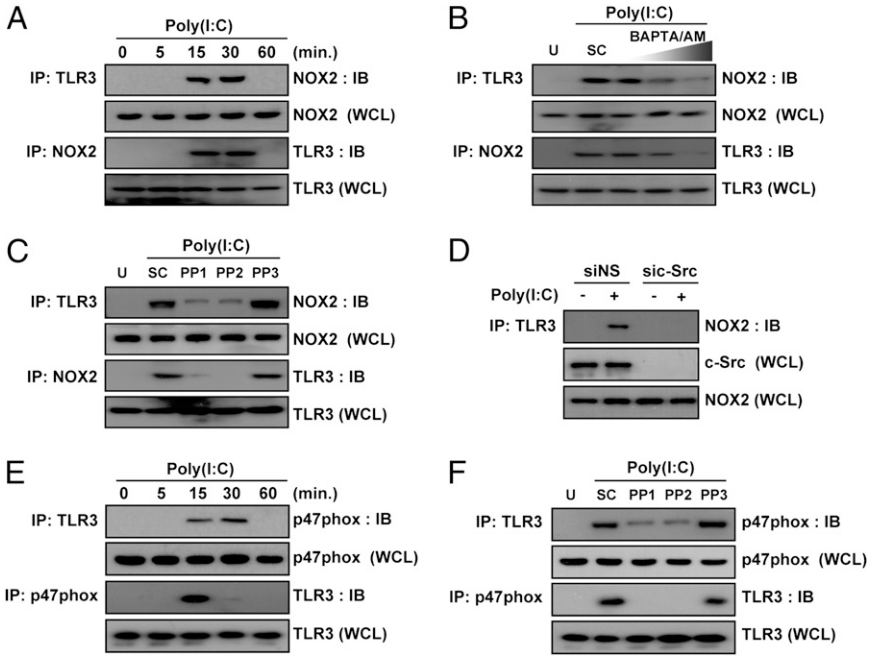

FIGURE 3. TLR3 interacts with NOX2 and p47^{phox} through intracellular Ca^{2+}–dependent c-Src kinase activation. (**A**–**C**) RAW264.7 cells were stimulated with poly(I:C) (25 μg/ml) for the indicated lengths of time and then subjected to immunoprecipitation (IP) with anti-TLR3 or anti-NOX2 Abs. RAW264.7 cells were preincubated with BAPTA-AM (5, 10, or 25 μM) for 45 min (B) or PP1 (10 μM), PP2 (10 μM), or PP3 (10 μM) for 45 min (C) and then stimulated with poly(I:C) for 30 min. Cells were then subjected to IP with anti-TLR3 or anti-NOX2 Abs. Protein interactions between NOX2 and TLR3 were analyzed by immunoblotting (IB) with anti-NOX2 and anti-TLR3 Abs. Whole-cell lysates (input control for TLR3 or NOX2) were detected by IB with anti-NOX2 and anti-TLR3 Abs. (**D**) RAW264.7 cells were transfected with siRNA targeting of *c-Src* (sic-Src) or siNS using Lipofectamine 2000. At 48 h after transfection, the cells were stimulated with poly(I:C) for 30 min and then subjected to IP with anti-TLR3 Ab. Protein interactions were analyzed by IB with anti-NOX2 Ab. Whole-cell lysates (input control for c-Src or NOX2) were detected by IB with anti-NOX2 and anti-TLR3 Abs. (**E** and **F**) TLR3 interacts with p47^{phox} through c-Src kinase activation. (E) RAW264.7 cells were stimulated with poly(I:C) (25 μg/ml) for the indicated lengths of time. (**F**) RAW264.7 cells were preincubated with PP1 (10 μM), PP2 (10 μM), or PP3 (10 μM) for 45 min and then stimulated with poly(I:C) for 30 min. Cells were then subjected to IP with anti-TLR3 or anti-p47^{phox} Abs. Protein interactions between p47^{phox} and TLR3 were analyzed by IB with anti-p47^{phox} and anti-TLR3 Abs. Whole-cell lysates (input control for p47^{phox} or TLR3) were detected by IB with anti-p47^{phox} and anti-TLR3 Abs. Data (A–F) are representative of at least three independent experiments with similar results. SC, Solvent control (0.1% DMSO); U, untreated.

Because p47^{phox} is an essential cytosolic component of the activated NOX complex (23), we next investigated whether TLR3 is associated with p47^{phox} in an Src-dependent manner in coimmunoprecipitation assays. In RAW264.7 macrophages, TLR3 was indeed associated with p47^{phox} (Fig. 3E), and the interaction between p47^{phox} and TLR3 was significantly diminished by pharmacologic inhibitors of c-Src kinases (PP1 and PP2) (Fig. 3F). Taken together, these results indicate that the poly(I:C)-induced interaction between TLR3 and NOX components (NOX2 and p47^{phox}) is mediated by intracellular Ca^{2+}–dependent c-Src activation.

TLR3-dependent ROS generation is required for the phosphorylation and nuclear translocation of STAT1 and STAT2

The transcription factor STAT1 plays an essential role in innate and inflammatory responses to type I and type II IFNs (24, 25). We first examined whether stimulation of TLR3 by poly(I:C) induces the phosphorylation of STAT1 at Tyr^{701} and Ser^{727} in BMDMs. As shown in Fig. 4A, poly(I:C) stimulation of BMDMs led to transient phosphorylation of STAT1 at Tyr^{701} and Ser^{727}. The response peaked within 2 h of poly(I:C) stimulation; phosphorylation thereafter declined to basal levels within 8 h (Fig. 4A). We also examined whether NOX-dependent ROS generation is required for STAT1 activation. Notably, poly(I:C)-induced phosphorylation of STAT1 at Tyr^{701} and Ser^{727} was markedly decreased in BMDMs from NOX2 and p47^{phox} KO mice compared with that from WT mice (Fig. 4B). Furthermore, STAT1 was actively translocated into the nucleus from 2 h after poly(I:C) stimulation (Supplemental Fig. 1A). The poly(I:C)-induced nuclear translocation of STAT1 was significantly reduced in BMDMs from NOX2 and p47^{phox} KO mice (Fig. 4C). Consistent with this, pretreatment of BMDMs with the ROS scavenger NAC and DPI significantly inhibited the poly(I:C)-induced nuclear translocation of STAT1 (Supplemental Fig. 1B).

Similar to STAT1, STAT2 is a key player in cellular responses to type I IFN (26). Thus, we examined whether TLR3 stimulation would activate STAT2 phosphorylation through intracellular ROS generation. As shown in Fig. 4D, stimulation of human monocytic THP-1 cells with poly(I:C) robustly induced the phosphorylation of STAT2 at Tyr^{690}. Poly(I:C)-induced STAT2 phosphorylation was dose-dependently attenuated by NAC and DPI, but not by the xanthine oxidase inhibitor allopurinol (Fig. 4E). Additionally, poly(I:C) stimulation induced the nuclear translocation of STAT2 in THP-1 cells, a response that was significantly inhibited by DPI (Fig. 4F).

We further questioned whether TLR3-induced type I IFN is involved in the activation of STAT proteins. To address this, BMDMs were treated with a neutralizing anti–IFN-α/β mAb (for 1 h) and then stimulated with poly(I:C). As shown in Fig. 4G, the phosphorylation of STAT1 at Tyr^{701} was slightly attenuated, and the phosphorylation of STAT1 at Ser^{727} was significantly reduced by pretreatment with anti–IFN-α/β mAb, compared with BMDMs treated with an isotype-matched control Ab (Fig. 4G). Taken together, these results indicate that NOX-dependent ROS generation is required for poly(I:C)-induced STAT1 and STAT2 activation through an autocrine type I IFN pathway.

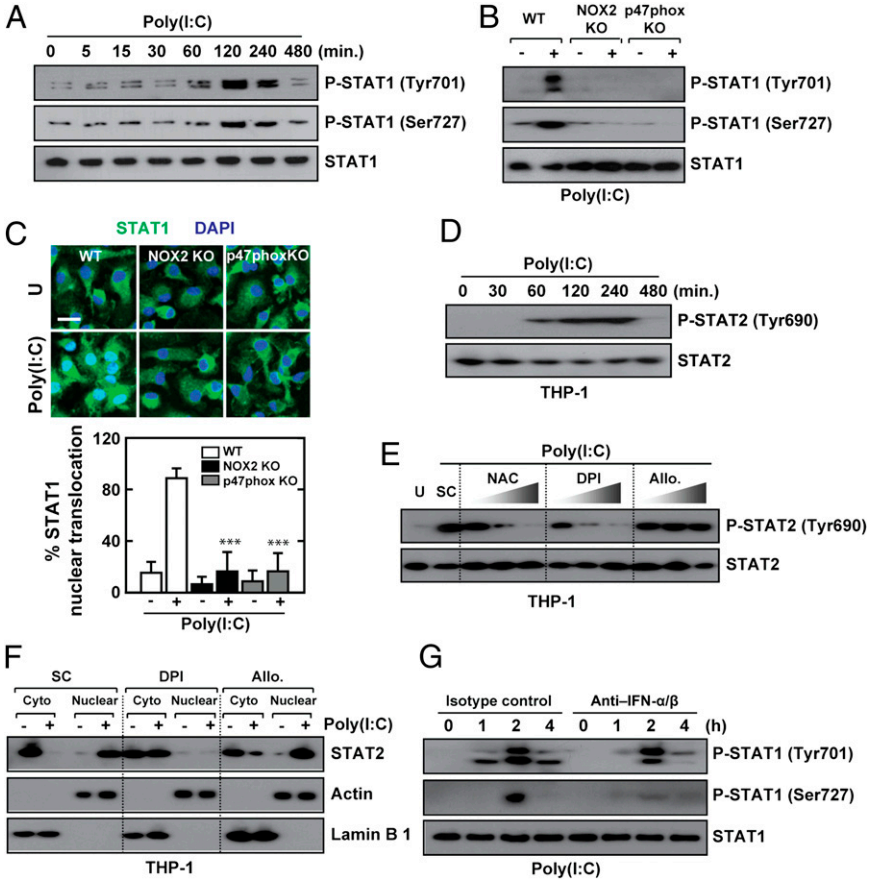

FIGURE 4. Poly(I:C)-induced ROS generation is required for the activation and nuclear translocation of STAT1 and STAT2. (**A** and **B**) Poly(I:C)-induced STAT1 activation. BMDMs were stimulated with poly(I:C) (25 μg/ml) for the indicated lengths of time (A). BMDMs were isolated from WT, NOX2 KO, and p47^{phox} KO mice and stimulated with poly(I:C) (25 μg/ml) for 2 h (B). The cells were then harvested and subjected to immunoblotting (IB) using anti–phospho-STAT1 and anti-STAT1 Abs (the latter for normalization). (**C**) BMDMs from WT, NOX2 KO, and p47^{phox} KO mice were stimulated with poly(I:C) for 2 h and then harvested for immunofluorescence microscopy. The cells were fixed, stained with anti-STAT1 Ab and DAPI, and examined under a confocal microscope. Scale bar, 20 μm. *Bottom*, Quantitative analysis of the nuclear translocation of STAT1. (**D** and **E**) Poly(I:C)-induced STAT2 activation. THP-1 cells were stimulated with poly(I:C) for the indicated lengths of time (D) or with poly(I:C) for 2 h in the presence or absence of NAC (10, 20, or 30 mM), DPI (10, 20, or 50 μM), or allopurinol (Allo; 0.01, 0.1, or 1 mM) for 45 min (E). (**F**) THP-1 cells were stimulated with poly(I:C) for 2 h in the presence or absence of DPI (20 μM) and allopurinol (Allo; 20 μM) for 45 min. Cytoplasmic and nuclear proteins were isolated using a nuclear extract kit, as described in *Materials and Methods*, and were subjected to IB analysis of STAT2 translocation. The same blots were washed and blotted for actin as a cytoplasmic marker and lamin B1 as a nuclear marker. (**G**) BMDMs were preincubated with anti–IFN-α/β or isotype control mAb (1 μg/ml) for 1 h and then stimulated with poly(I:C) for the indicated lengths of time. Cells were then harvested and subjected to IB with anti–phospho-STAT1 and anti-STAT1 Abs (the latter for normalization). The data (A–G) are representative of at least three independent experiments with similar results. SC, Solvent control (0.1% DMSO); U, untreated.

TLR3-dependent ROS generation is required for NF-κB and IRF-3 activation

TLR3 signaling activates the transcription factors NF-κB and IRF-3, inducing production of the proinflammatory cytokines TNF-α and IFN-β, respectively (27, 28). We next examined whether ROS generation is involved in the nuclear translocation and activation of NF-κB and IRF-3 after stimulation with poly(I:C). The nuclear translocation of NF-κB and IRF-3 peaked at 1 and 3 h, respectively (data not shown). Poly(I:C)-induced translocation of endogenous NF-κB p65 into the nucleus (assessed by immunofluorescence) was reduced in NOX2- and p47^{phox}-deficient BMDMs compared with WT cells (Fig. 5A). Similar inhibition of the poly(I:C)-induced translocation of NF-κB p65 into the nucleus was observed in macrophages subjected to ROS scavenger and NOX inhibitor treatment (Supplemental Fig. 2A). Additionally, poly(I:C)-induced NF-κB DNA-binding activity was markedly reduced in NOX2- and p47^{phox}-deficient BMDMs (Fig. 5B). Consistent with this, poly(I:C)-induced NF-κB DNA-binding activity was markedly reduced by pretreatment with antioxidants (NAC, 4-(2-aminoethyl)-benzenesulfonyl fluoride hydrochloride, and pyrrolidine dithiocarbamate ammonium) and DPI, but not the xanthine oxidase inhibitor allopurinol (Supplemental Fig. 2B). In TLR stimulation, activation of the three-subunit inhibitor of the NF-κB kinase (IKKα/β/γ) complex and phosphorylation of IκB-α are crucial for the translocation of NF-κB dimers into the nucleus (29). Consistent with the results for the nuclear translocation of NF-κB, poly(I:C)-induced activation of IKKα/β and IκB-α degradation was abrogated in BMDMs from NOX2 and p47^{phox} KO mice compared with WT mice (Fig. 5C).

Furthermore, we found that the poly(I:C)-induced nuclear translocation of IRF-3 was significantly inhibited in BMDMs from NOX2 and p47^{phox} KO mice compared with those from WT mice (Fig. 5D). Moreover, poly(I:C)-induced nuclear translocation of IRF-3 in BMDMs was dramatically reduced by pretreatment with NAC and DPI, but not allopurinol (Supplemental Fig. 2C). We also quantified the DNA-binding activity of IRF-3 using an ELISA-based assay. The level of IRF-3 DNA binding was significantly attenuated in BMDMs from NOX2 and p47^{phox} KO

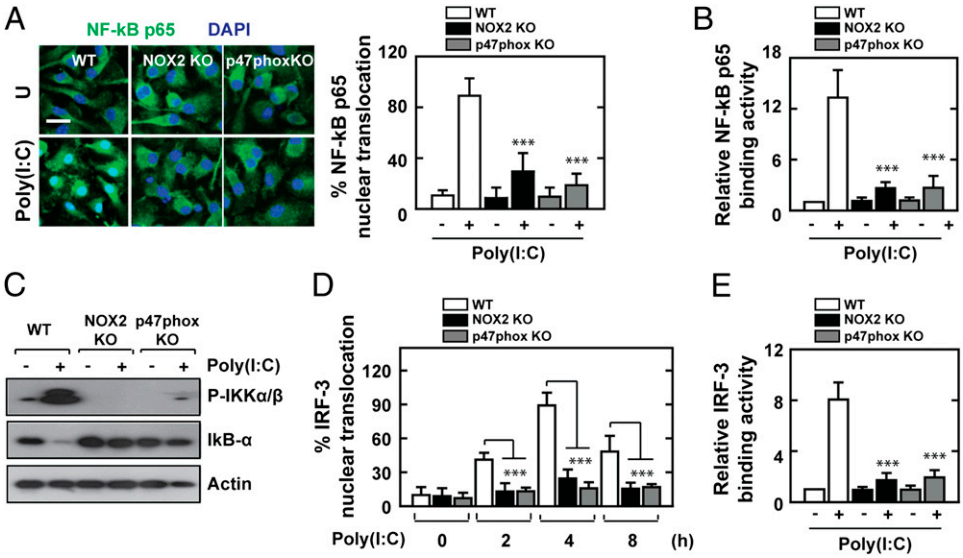

FIGURE 5. Poly(I:C)-induced activation of NF-κB and IRF-3 is dependent on intracellular ROS generation. (**A**) Assessment of NF-κB nuclear translocation. BMDMs from WT, NOX2 KO, and p47^{phox} KO mice were stimulated with poly(I:C) for 1 h. The cells were fixed and stained with anti–NF-κB p65 Ab and DAPI, and were then examined under a confocal microscope. Scale bar, 20 μm. *Right*, Quantitative analysis of the nuclear translocation of NF-κB p65. (**B**) Assessment of NF-κB DNA binding activity. BMDMs from WT, NOX2 KO, and p47^{phox} KO mice were stimulated with poly(I:C) for 1 h. NF-κB DNA-binding activity in nuclear extracts (5 μg protein) was assessed using Trans-AM transcription factor assay kits, as described in *Materials and Methods*. (**C**) The experimental conditions were the same as in (A). The cells were harvested and subjected to immunoblotting for phosphorylated IKKα/β or IκB-α. The same blots were then washed and blotted for actin as a loading control. (**D**) The experimental conditions were the same as in (A). The cells were fixed and stained with anti–IRF-3 Ab and DAPI and then examined under a confocal microscope. Quantitative analysis of the nuclear translocation of IRF-3 is shown. (**E**) Assessment of IRF-3 DNA-binding activity. The experimental conditions were the same as in (B). Data (A, *left*, C) are representative of five independent experiments with similar results. The quantitative data (A, *right*, B, D, E) are shown as the means ± SD of three experiments. ***$p <$ 0.001, compared with the solvent control. U, Untreated.

mice compared with those from WT mice (Fig. 5E). Taken together, these data suggest that TLR3-induced ROS are important for the activation of the transcription factors NF-κB and IRF-3.

TLR3-induced STAT1 activation is required for the expression of CXCL10, CCL5, IFN-β, and inducible NO synthase in BMDMs

TLR3-dependent IRF-3 activation results in type I IFN production and the subsequent induction of IFN-responsive genes such as CXCL10 (5, 6). Type I IFN–dependent biological effects are mediated through activation of the JAK/STAT pathway (7). We thus investigated the roles of NOX2, p47^{phox}, and STAT1 in the poly(I:C)-induced production of inflammatory chemokines and inducible NO synthase (iNOS). As shown in Fig. 6A, poly(I:C)-induced CXCL10 and CCL5 mRNA synthesis was significantly reduced in STAT1 KO macrophages. Additionally, poly(I:C)-induced iNOS expression and nitrite synthesis were markedly reduced in STAT1 KO macrophages and in siRNA targeting of STAT1-transfected RAW264.7 cells (Fig. 6A–C). Furthermore, poly(I:C)-induced expression of CXCL10, CCL5, IFN-β, and iNOS (Fig. 6D) and nitrite production (Fig. 6E) were markedly decreased in NOX2- and p47^{phox}-deficient macrophages compared with WT cells. Poly(I:C)-induced TNF-α production was also substantially decreased in NOX2- and p47^{phox}-deficient macrophages compared with WT cells (Fig. 6D). These data show that macrophage expression of IRF-3–inducible genes requires STAT1 activation and the expression of NOX2 and p47^{phox}.

Discussion

Innate immune responses triggered by TLR signaling are mediated through generation of intracellular ROS, which are now being recognized as important second messengers (13, 30). Previously, it was suggested that NOX2-dependent ROS generation is required for TLR2-dependent inflammatory responses in macrophages (16). Bae et al. (19) showed that minimally oxidized low-density lipoprotein-dependent ROS generation catalyzed by NOX2 involves a TLR4-dependent pathway and plays a role in the production of RANTES and migration of smooth-muscle cells. Our findings indicate a broader role for ROS in TLR3-dependent inflammatory mediator expression by macrophages. Poly(I:C)-induced ROS generation was diminished in TLR3 KO macrophages, and the TLR3 adaptor TRIF could play a role in poly(I:C)-mediated ROS generation. Our data partially correlate with previous studies showing that ROS can mediate lung injury and inflammatory cytokine production by lung macrophages via a TLR4-TRIF–dependent pathway (30). Additionally, a recent study showed that MyD88, a well-characterized TLR adaptor, is essential for lactic acid bacteria–induced ROS generation, which is primarily catalyzed by NADPH oxidase, and IL-12 production (31). Thus, TLR signaling and key adaptors may play pivotal roles in innate immune signaling through ROS generation. Our demonstration that the TLR3/TRIF axis, but not RIG-I or MDA5, is required for dsRNA-induced ROS generation and downstream signaling is unique.

Our results indicate that NOX2 is an important source of TLR3-induced ROS and that the essential components of NOX enzyme complex (NOX2 and p47^{phox}) bind to TLR3 to initiate an intracellular signaling cascade. In terms of the role of ROS as modulators of cellular signaling and gene regulation, NOX enzymes are regarded to be a key source of cellular ROS in a variety of cells (15, 30, 32). Previous studies showed that NOX2-derived ROS are required for efficient RIG-I–mediated IRF-3 activation and expression of the antiviral cytokine IFN-β (33). Additionally, NOX2 plays an important role in the expression of the mitochondria-associated adaptor MAVS (33). In dendritic cells, NOX2-dependent ROS negatively regulate IL-12 expression by attenuating p38-MAPK activity (32). Furthermore, recent studies have shown

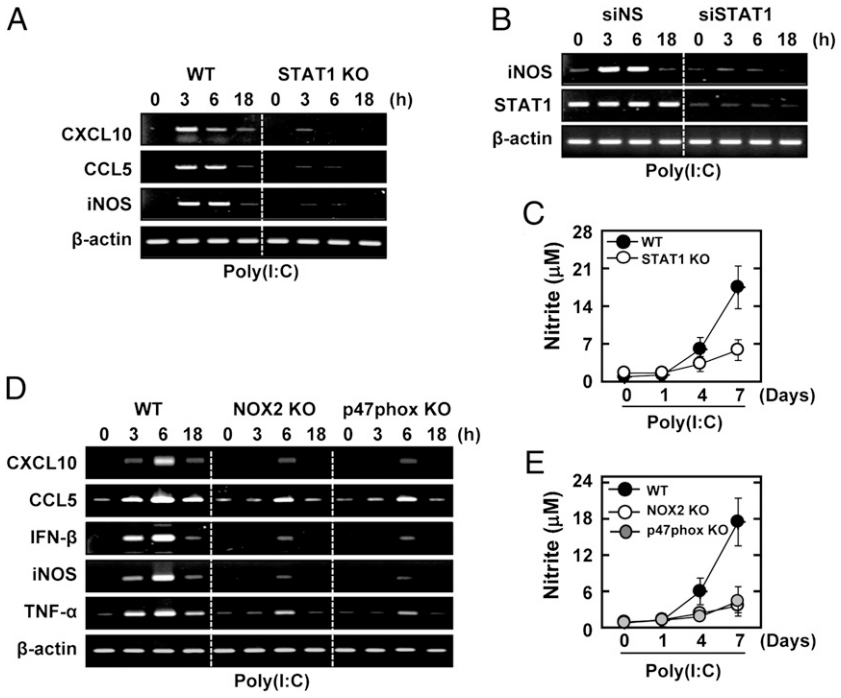

FIGURE 6. Poly(I:C)-induced production of chemokines and iNOS is dependent on the expression of STAT1, NOX2, and p47^{phox}. (**A**) BMDMs from WT and STAT1 KO mice were stimulated with poly(I:C) (25 μg/ml) for the indicated lengths of time. Cells were then harvested and subjected to semiquantitative RT-PCR for CXCL10, CCL5, and iNOS. The β-actin mRNA level was used as a loading control. (**B**) Semiquantitative RT-PCR analysis of iNOS mRNA expression in siRNA targeting of STAT1 (siSTAT1)-transfected RAW264.7 cells stimulated with poly(I:C) for the indicated lengths of time. The efficacy of the siSTAT1 is shown. The mRNA loading was normalized according to β-actin expression in cells. (**C**) The kinetics of poly(I:C)-induced nitrite production in BMDMs from WT and STAT1 KO mice. (**D** and **E**) Poly(I:C)-induced CXCL10, CCL5, IFN-β, iNOS, and TNF-α mRNA expression (D) and nitrite production (E) in peritoneal macrophages from WT, NOX2 KO, and p47^{phox} KO mice. Data (A, B, D) are representative of five independent experiments with similar results. The results of densitometric analysis of data from five experiments (mean ± SD) are shown (C, E).

that the NOX isozyme dual oxidase 2 is critically involved in TLR5-induced innate immune responses, manifested by IL-8 production and mucin generation in human nasal epithelial cells and mice (34). Tang et al. (35) further suggested that ROS play an important role in the initiation and orchestration of Th type 2 responses to cysteine proteases. It has been suggested that there is also a connection between innate signaling and mitochondrial ROS, which also play a crucial role in killing intracellular bacteria in response to stimulation of TLR1, TLR2, and TLR4 (36). In this study, we focused on the role of NOX-derived cellular ROS; however, future studies will clarify the roles of mitochondrial ROS in TLR3-induced inflammatory responses. Taken together, these data reveal a new facet of the role of NOX2-derived ROS, which tailor regulation of innate host immune responses initiated by pattern recognition receptors and bridging adaptive immunity.

Poly(I:C)-induced Src phosphorylation and intracellular Ca^{2+} influx appear to be important for TLR3-mediated ROS generation owing to their regulation of the TLR3-NOX2 and p47^{phox} interaction in macrophages. Previous studies have shown that TLR3 is translocated to endosomes in response to dsRNA and colocalizes with c-Src on endosomes containing dsRNA in human monocyte-derived dendritic cells (21). dsRNA-induced activation of IRF-3 and STAT1 is dependent on c-Src kinase (21). Furthermore, Src family kinases play important roles as receptor-proximal regulators of TLR tyrosine phosphorylation and signaling (21, 37). Ca^{2+} is a second messenger in many cellular signaling cascades, including T and B cell receptor cascades (38, 39). Calcium signaling also seems to play a central role in TLR signaling because TLR2 ligands stimulate calcium influx via c-Src activation, further recruiting PI3K and phospholipase Cγ and resulting in enhanced calcium release in airway epithelial cells (22, 40). Taken together, these data strongly suggest that intracellular Ca^{2+}–induced Src kinase activation is essential for the initiation of innate signaling pathways through NOX-dependent ROS generation.

We showed in this study that TLR3-induced ROS are essential for the generation of innate and inflammatory mediators, such as NO, cytokines, and chemokines, through STAT1 activation. The transcription factor STAT1 is an important cytoplasmic molecule involved in cellular responses and signaling cascades initiated by type I IFNs (41). When cells are exposed to these cytokines, or stress signals, STAT1 can be phosphorylated on Tyr^{701} and Ser^{727} and translocates to the nucleus, where it regulates the expression of various genes involved in innate immune responses and inflammation, including those encoding iNOS (26) and various inflammatory cytokines and chemokines (42). Recent studies showed that inflammatory responses in the cochlea are mediated through activation of STAT1, which requires the generation of ROS by NOX3 (43). We also showed that the phosphorylation of STAT1 was modulated by pretreatment with anti–IFN-α/β mAb, indicating that poly(I:C)-induced STAT1 activation is mediated through an autocrine type I IFN pathway. Moreover, poly(I:C)-induced phosphorylation and nuclear translocation of STAT2, a key player in responses to type I IFN (26), was dependent on ROS signaling. Thus, the observation that ROS control STAT1/STAT2 phosphorylation and STAT1-mediated inflammatory activation provides evidence of a vital role for NOX-dependent ROS signaling in TLR3-mediated innate immune activation in macrophages.

Our data partly correlate with previous in vitro studies showing that synthesis of poly(I:C)-stimulated TNF-α and IFN-β is significantly decreased in BMDMs from p47^{phox} KO mice as compared with those from WT mice (28). Additionally, it was shown that dual oxidase 1 is involved in TLR ligand–induced IL-8 and VEGF production in airway epithelial cells (44). These studies, together with findings in the present study, strongly suggest that TLRs and ROS regulate inflammatory responses in a cell type–specific manner. Patients with chronic granulomatous disease (CGD) in infancy or childhood often suffer from life-threatening bacterial and fungal infections (45, 46); however, it is not known whether susceptibility to viral infections is increased in CGD patients. Recent studies have shown that CGD patients maintain an intact memory response in humoral immunity, with normal serum IgG and influenza-specific Ab levels, although they have reduced numbers of circulating CD27^{+} memory B cells (47). Moreover, NOX2-deficient T cells show a skewed Th1 response, with augmented IFN-γ and decreased IL-4 production (48). These data collectively suggest that intact, and perhaps augmented, adaptive immune responses (i.e., humoral immunity and Th1 inflammatory responses) may compensate for the profound innate

immune defect and contribute to enhanced responses to influenza virus infection in CGD patients and animal models.

In conclusion, we provide evidence of a critical role for NOX2-dependent ROS in regulating TLR3-mediated innate immune responses in macrophages. NOX2 and $p47^{phox}$ interact with TLR3 to activate inflammatory responses; this is regulated by intracellular calcium-Src activation. TLR3-induced ROS generation is essential for STAT1 activation, which plays a key role in inflammatory mediator release. These observations reveal a new role for NOX in regulating innate immune responses triggered by TLR3 engagement. The vital role of NOX-derived ROS in regulating TLR3-induced innate immune responses suggests that modulating ROS functions may represent a novel therapeutic strategy for the treatment of infections and inflammatory disorders.

Acknowledgments

We thank Dr. Y.S. Bae (Ewha University, Seoul, South Korea) for provision of NOX2 KO mice, Dr. I. Flavel (Yale University, New Haven, CT) for provision of TLR3 KO mice, Dr. S. Akira (Osaka University, Osaka, Japan) for provision of TRIF KO mice, Dr. G.M. Hur (Chungnam National University) for provision of NF-κB luciferase reporter plasmid, J.M. Yuk and H.M. Lee (Chungnam National University) for critical reading of the manuscript, and H.S. Jin (Chungnam National University) for excellent technical assistance.

Disclosures

The authors have no financial conflicts of interest.

References

1. Alexopoulou, L., A. C. Holt, R. A. Medzhitov, and R. A. Flavell. 2001. Recognition of double-stranded RNA and activation of NF-κB by Toll-like receptor 3. *Nature* 413: 732–738.
2. Akira, S., K. Takeda, and T. Kaisho. 2001. Toll-like receptors: critical proteins linking innate and acquired immunity. *Nat. Immunol.* 2: 675–680.
3. Yamamoto, M., S. Sato, H. Hemmi, K. Hoshino, T. Kaisho, H. Sanjo, O. Takeuchi, M. Sugiyama, M. Okabe, K. Takeda, and S. Akira. 2003. Role of adaptor TRIF in the MyD88-independent Toll-like receptor signaling pathway. *Science* 301: 640–643.
4. Takeuchi, O., and S. Akira. 2009. Innate immunity to virus infection. *Immunol. Rev.* 227: 75–86.
5. Weighardt, H., G. Jusek, J. Mages, R. Lang, K. Hoebe, B. Beutler, and B. Holzmann. 2004. Identification of a TLR4- and TRIF-dependent activation program of dendritic cells. *Eur. J. Immunol.* 34: 558–564.
6. Akira, S., S. Uematsu, and O. Takeuchi. 2006. Pathogen recognition and innate immunity. *Cell* 124: 783–801.
7. van Boxel-Dezaire, A. H., M. R. Rani, and G. R. Stark. 2006. Complex modulation of cell type-specific signaling in response to type I interferons. *Immunity* 25: 361–372.
8. Gao, J. J., M. B. Filla, M. J. Fultz, S. N. Vogel, S. W. Russell, and W. J. Murphy. 1998. Autocrine/paracrine IFN-αβ mediates the lipopolysaccharide-induced activation of transcription factor Stat1α in mouse macrophages: pivotal role of Stat1α in induction of the inducible nitric oxide synthase gene. *J. Immunol.* 161: 4803–4810.
9. Kim, H. S., and M. S. Lee. 2005. Essential role of STAT1 in caspase-independent cell death of activated macrophages through the p38 mitogen-activated protein kinase/STAT1/reactive oxygen species pathway. *Mol. Cell. Biol.* 25: 6821–6833.
10. Schindler, C., and J. E. Darnell, Jr. 1995. Transcriptional responses to polypeptide ligands: the JAK-STAT pathway. *Annu. Rev. Biochem.* 64: 621–651.
11. Saha, B., S. Jyothi Prasanna, B. Chandrasekar, and D. Nandi. 2010. Gene modulation and immunoregulatory roles of interferon γ. *Cytokine* 50: 1–14.
12. Najjar, I., F. Baran-Marszak, C. Le Clorennec, C. Laguillier, O. Schischmanoff, I. Youlyouz-Marfak, M. Schlee, G. W. Bornkamm, M. Raphaël, J. Feuillard, and R. Fagard. 2005. Latent membrane protein 1 regulates STAT1 through NF-κB-dependent interferon secretion in Epstein-Barr virus-immortalized B cells. *J. Virol.* 79: 4936–4943.
13. Forman, H. J., and M. Torres. 2002. Reactive oxygen species and cell signaling: respiratory burst in macrophage signaling. *Am. J. Respir. Crit. Care Med.* 166: S4–S8.
14. Lam, G. Y., J. Huang, and J. H. Brumell. 2010. The many roles of NOX2 NADPH oxidase-derived ROS in immunity. *Semin. Immunopathol.* 32: 415–430.
15. Bae, Y. S., H. Oh, S. G. Rhee, and Y. D. Yoo. 2011. Regulation of reactive oxygen species generation in cell signaling. *Mol. Cells* 32: 491–509.
16. Yang, C. S., D. M. Shin, K. H. Kim, Z. W. Lee, C. H. Lee, S. G. Park, Y. S. Bae, and E. K. Jo. 2009. NADPH oxidase 2 interaction with TLR2 is required for efficient innate immune responses to mycobacteria via cathelicidin expression. *J. Immunol.* 182: 3696–3705.
17. Matsuzawa, A., K. Saegusa, T. Noguchi, C. Sadamitsu, H. Nishitoh, S. Nagai, S. Koyasu, K. Matsumoto, K. Takeda, and H. Ichijo. 2005. ROS-dependent activation of the TRAF6-ASK1-p38 pathway is selectively required for TLR4-mediated innate immunity. *Nat. Immunol.* 6: 587–592.
18. Yang, C. S., D. S. Lee, C. H. Song, S. J. An, S. Li, J. M. Kim, C. S. Kim, D. G. Yoo, B. H. Jeon, H. Y. Yang, et al. 2007. Roles of peroxiredoxin II in the regulation of proinflammatory responses to LPS and protection against endotoxin-induced lethal shock. *J. Exp. Med.* 204: 583–594.
19. Yang, C. S., D. M. Shin, H. M. Lee, J. W. Son, S. J. Lee, S. Akira, M. A. Gougerot-Pocidalo, J. El-Benna, H. Ichijo, and E. K. Jo. 2008. ASK1-p38 MAPK-p47phox activation is essential for inflammatory responses during tuberculosis via TLR2-ROS signalling. *Cell Microbiol.* 10: 741–754.
20. Kato, H., O. Takeuchi, S. Sato, M. Yoneyama, M. Yamamoto, K. Matsui, S. Uematsu, A. Jung, T. Kawai, K. J. Ishii, et al. 2006. Differential roles of MDA5 and RIG-I helicases in the recognition of RNA viruses. *Nature* 441: 101–105.
21. Johnsen, I. B., T. T. Nguyen, M. Ringdal, A. M. Tryggestad, O. Bakke, E. Lien, T. Espevik, and M. W. Anthonsen. 2006. Toll-like receptor 3 associates with c-Src tyrosine kinase on endosomes to initiate antiviral signaling. *EMBO J.* 25: 3335–3346.
22. Chun, J., and A. Prince. 2006. Activation of Ca^{2+}-dependent signaling by TLR2. *J. Immunol.* 177: 1330–1337.
23. El-Benna, J., P. M. Dang, M. A. Gougerot-Pocidalo, J. C. Marie, and F. Braut-Boucher. 2009. $p47^{phox}$, the phagocyte NADPH oxidase/NOX2 organizer: structure, phosphorylation and implication in diseases. *Exp. Mol. Med.* 41: 217–225.
24. Durbin, J. E., T. R. Johnson, R. K. Durbin, S. E. Mertz, R. A. Morotti, R. S. Peebles, and B. S. Graham. 2002. The role of IFN in respiratory syncytial virus pathogenesis. *J. Immunol.* 168: 2944–2952.
25. Hu, X., S. D. Chakravarty, and L. B. Ivashkiv. 2008. Regulation of interferon and Toll-like receptor signaling during macrophage activation by opposing feedforward and feedback inhibition mechanisms. *Immunol. Rev.* 226: 41–56.
26. Stempelj, M., M. Kedinger, L. Augenlicht, and L. Klampfer. 2007. Essential role of the JAK/STAT1 signaling pathway in the expression of inducible nitric-oxide synthase in intestinal epithelial cells and its regulation by butyrate. *J. Biol. Chem.* 282: 9797–9804.
27. Oshiumi, H., M. Matsumoto, K. Funami, T. Akazawa, and T. Seya. 2003. TICAM-1, an adaptor molecule that participates in Toll-like receptor 3-mediated interferon-beta induction. *Nat. Immunol.* 4: 161–167.
28. Seleme, M. C., W. Lei, A. R. Burg, K. Y. Goh, A. Metz, C. Steele, and H. M. Tse. 2012. Dysregulated TLR3-dependent signaling and innate immune activation in superoxide-deficient macrophages from nonobese diabetic mice. *Free Radic. Biol. Med.* 52: 2047–2056.
29. Yuk, J. M., and E. K. Jo. 2011. Toll-like receptors and innate immunity. *J. Bacteriol. Virol.* 41: 225–235.
30. Imai, Y., K. Kuba, G. G. Neely, R. Yaghubian-Malhami, T. Perkmann, G. van Loo, M. Ermolaeva, R. Veldhuizen, Y. H. Leung, H. Wang, et al. 2008. Identification of oxidative stress and Toll-like receptor 4 signaling as a key pathway of acute lung injury. *Cell* 133: 235–249.
31. Ichikawa, S., M. Miyake, R. Fujii, and Y. Konishi. 2012. MyD88 associated ROS generation is crucial for *Lactobacillus* induced IL-12 production in macrophage. *PLoS ONE* 7: e35880.
32. Jendrysik, M. A., S. Vasilevsky, L. Yi, A. Wood, N. Zhu, Y. Zhao, S. M. Koontz, and S. H. Jackson. 2011. NADPH oxidase-2 derived ROS dictates murine DC cytokine-mediated cell fate decisions during CD4 T helper-cell commitment. *PLoS ONE* 6: e28198.
33. Soucy-Faulkner, A., E. Mukawera, K. Fink, A. Martel, L. Jouan, Y. Nzengue, D. Lamarre, C. Vande Velde, and N. Grandvaux. 2010. Requirement of NOX2 and reactive oxygen species for efficient RIG-I-mediated antiviral response through regulation of MAVS expression. *PLoS Pathog.* 6: e1000930.
34. Joo, J. H., J. H. Ryu, C. H. Kim, H. J. Kim, M. S. Suh, J. O. Kim, S. Y. Chung, S. N. Lee, H. M. Kim, Y. S. Bae, and J. H. Yoon. 2012. Dual oxidase 2 is essential for the Toll-like receptor 5-mediated inflammatory response in airway mucosa. *Antioxid. Redox Signal.* 16: 57–70.
35. Tang, H., W. Cao, S. P. Kasturi, R. Ravindran, H. I. Nakaya, K. Kundu, N. Murthy, T. B. Kepler, B. Malissen, and B. Pulendran. 2010. The T helper type 2 response to cysteine proteases requires dendritic cell-basophil cooperation via ROS-mediated signaling. *Nat. Immunol.* 11: 608–617.
36. West, A. P., I. E. Brodsky, C. Rahner, D. K. Woo, H. Erdjument-Bromage, P. Tempst, M. C. Walsh, Y. Choi, G. S. Shadel, and S. Ghosh. 2011. TLR signalling augments macrophage bactericidal activity through mitochondrial ROS. *Nature* 472: 476–480.
37. Medvedev, A. E., W. Piao, J. Shoenfelt, S. H. Rhee, H. Chen, S. Basu, L. M. Wahl, M. J. Fenton, and S. N. Vogel. 2007. Role of TLR4 tyrosine phosphorylation in signal transduction and endotoxin tolerance. *J. Biol. Chem.* 282: 16042–16053.
38. Gardner, P. 1989. Calcium and T lymphocyte activation. *Cell* 59: 15–20.
39. Gallo, E. M., K. Canté-Barrett, and G. R. Crabtree. 2006. Lymphocyte calcium signaling from membrane to nucleus. *Nat. Immunol.* 7: 25–32.
40. Chun, J., and A. Prince. 2009. Ca^{2+} signaling in airway epithelial cells facilitates leukocyte recruitment and transepithelial migration. *J. Leukoc. Biol.* 86: 1135–1144.
41. Stark, G. R., and J. E. Darnell, Jr. 2012. The JAK-STAT pathway at twenty. *Immunity* 36: 503–514.
42. Wagner, A. H., I. Wittjen, T. Stojanovic, P. Middel, J. G. Meingassner, and M. Hecker. 2008. Signal transducer and activator of transcription 1 decoy oligodeoxynucleotide suppression of contact hypersensitivity. *J. Allergy Clin. Immunol.* 121: 158–165, e5.
43. Kaur, T., D. Mukherjea, K. Sheehan, S. Jajoo, L. P. Rybak, and V. Ramkumar. 2011. Short interfering RNA against STAT1 attenuates cisplatin-induced ototoxicity in the rat by suppressing inflammation. *Cell Death Dis.* 2: e180.

44. Koff, J. L., M. X. Shao, I. F. Ueki, and J. A. Nadel. 2008. Multiple TLRs activate EGFR via a signaling cascade to produce innate immune responses in airway epithelium. *Am. J. Physiol. Lung Cell. Mol. Physiol.* 294: L1068–L1075.
45. Heyworth, P. G., A. R. Cross, and J. T. Curnutte. 2003. Chronic granulomatous disease. *Curr. Opin. Immunol.* 15: 578–584.
46. Assari, T. 2006. Chronic granulomatous disease; fundamental stages in our understanding of CGD. *Med. Immunol.* 5: 4.
47. Moir, S., S. S. De Ravin, B. H. Santich, J. Y. Kim, J. G. Posada, J. Ho, C. M. Buckner, W. Wang, L. Kardava, M. Garofalo, et al. 2012. Humans with chronic granulomatous disease maintain humoral immunologic memory despite low frequencies of circulating memory B cells. *Blood* 120: 4850–4858.
48. Shatynski, K. E., H. Chen, J. Kwon, and M. S. Williams. 2012. Decreased STAT5 phosphorylation and GATA-3 expression in NOX2-deficient T cells: role in T helper development. *Eur. J. Immunol.* 42: 3202–3211.